Comparison of Turbulence Models in Shock-Wave/ Boundary-Layer Interaction

Sang Dug Kim
Department of Aerospace Engineering, University of Illinois at Urbana-Champaign Urbana, IL 61801, USA
Chang Oh Kwon
Korea Institute of Industrial Technology, Incheon 404-254, Korea
Dong Joo Song*
School of Mechanical Engineering, Yeungnam University, Gyongsan 712-749, Korea

This paper presents a comparative study of a fully coupled, upwind, compressible Navier-Stokes code with three two-equation models and the Baldwin-Lomax algebraic model in predicting transonic/supersonic flow. The $k-\varepsilon$ turbulence model of Abe performed well in predicting the pressure distributions and the velocity profiles near the flow separation over the axisymmetric bump, even though there were some discrepancies with the experimental data in the shear-stress distributions. Additionally, it is noted that this model has y^* in damping functions instead of y^+. The turbulence model of Abe and Wilcox showed better agreements in skin friction coefficient distribution with the experimental data than the other models did for a supersonic compression ramp problem. Wilcox's model seems to be more reliable than the other models in terms of numerical stability. The two-equation models revealed that the redevelopment of the boundary layer was somewhat slow downstream of the reattachment portion.

Key Words : Turbulence Models, Shock-Wave/Boundary-Layer Interaction CSCM method, k-ε models of Abe, Bunpflow

Nomenclature

a : Sonic speed [m/s]
A : Jacobian matrix
c : Chord of bump [m]
C_f : Skin friction coefficient, $2\tau_w/\rho_\infty u_\infty^2$
e : Volumetric internal energy, $p/(\gamma-1)$ [N/m^2]
E : Volumetric total energy, $e+e(u^2+v^2)/2$ [N/m^2]
F, G : Flux vectors [kg/m^2·s]
h : The height of the bump
k : Turbulent kinetic energy [m^2/s^2]
κ : Von Karman constant
Ma : Mach number
p : Static pressure [N/m^2]
p_t : Total pressure [N/m^2]
Pr : Prandtl number
q : Conservative variables
$\tilde{q}$: Primitive variables
$\tilde{\tilde{q}}$: Characteristic variables
Re : Reynolds number
R_t : Turbulent Reynolds number, $\rho k^2/\mu\phi$
S : Source term vector
u, v : Cartesian velocity components [m/s]
u_τ : Friction velocity, $\sqrt{\tau_w/\rho}$ [m/s]
u_ε : Kolmogorov velocity scale, $(\mu\varepsilon/\rho)^{1/4}$ [m/s]
x, y : Cartesian coordinates [m]
y^+ : Dimensionless distance from the wall,

* Corresponding Author,
E-mail : djsong@yu.ac.kr
TEL : +82-53-810-2449; **FAX** : +82-53-813-3703
School of Mechanical Engineering, Yeungnam University, Gyongsan 712-749, Korea. (Manuscript **Received** February 5, 2003; **Revised** November 14, 2003)

$\rho u_\tau y/\mu$

y^* : Dimensionless distance from the wall, $\rho u_\varepsilon y/\mu$

Greek symbols

δ : Boundary-layer thickness [m]
γ : Specific heat ratio, =1.4
μ : Molecular viscosity [kg/m·s]
μ_t : Turbulent eddy viscosity [kg/m²·s]
ν : Kinematic viscosity [m/s]
ϕ : Dissipation rate of turbulent kinetic energy, ε, $\tilde{\varepsilon}$ [m²/s³], ω[1/s]
σ_k, σ_ϕ : Turbulent Prandtl numbers for k and ϕ
Δ : Forward difference in a direction
ξ, η : Generalized curvilinear coordinates

Subscripts

l : Laminar quantity
t : Turbulence quantity
w : Quantity at the wall
∞ : Freestream quantity
o : Quantity at the inlet

1. Introduction

The greatly improved processing capabilities of computers and efficient numerical algorithms made it possible to apply the Navier-Stokes equations with turbulence closure to complex compressible aerodynamic flow problems. The major areas of compressible flow applications have been shock-boundary layer and shock-shock interactions in transonic/supersonic flows over complex geometry. It is not easy to get an accurate surface pressure and skin friction coefficient distribution in transonic/supersonic flows with strong interactions between the inviscid and viscous flow regions or between the shock-wave and turbulent-boundary layer due to the complex nature of the flowfield. The distribution of pressure and skin friction can be affected by the location of the shock-wave, which strongly depends on the geometric shape, especially in supersonic flows and by the development of viscous flow regions which affect the resultant shock-wave location in transonic flows. Although the overall flowfield could be reasonably predicted, the prediction of the proper extent and size of the flow separation region and the accurate skin friction coefficient was extremely difficult. But these phenomena are easily found in many practical areas of fluid mechanics such as transonic/supersonic turbomachinery design and external aerodynamics over airfoil or wings.

An algebraic turbulence model is usually adopted for compressible Navier-Stokes codes, since it is easy to implement and requires minimum computer time and storage, which is of particular importance in three-dimensional computations. Baldwin and Lomax (1978) proposed an algebraic eddy viscosity model, patterned after that of Cebeci and Smith (1974). This model does not require the determination of the boundary layer edge, since it employs the vorticity that is an invariant under coordinate transformations. But it may not, in general, be valid for complex flows, because y^+ can be poorly defined near the flow separation zone where the wall shear stress is zero. Furthermore, as this model strongly depends on local vorticity, it often results in the oscillatory solution for length scales. Thus, turbulent shear layer calculations with an algebraic mixing length formulation produce discontinuous predictions of the eddy viscosity, which may deteriorate the mean flow calculation. Visbal and Knight (1984) carried out a comparative study of a modified model for upstream history effect and the original Baldwin-Lomax model for the supersonic compression corner problem. However, these models failed to predict the rapid recovery of boundary layer downstream of a reattachment point. Johnson and King (1985) proposed a nonequilibrium turbulence closure model in scrutinizing the transonic flows over an axisymmetric bump. It was started by using the Cebeci-Smith model (1974) and was turned on downstream from a specified streamwise station, ahead of the leading edge of the bump. The surface pressure distribution from this model agreed with the experimental data. Goldberg (1991) derived a one-equation model based on two time scales. The time scales of the small dissipative eddies are different from those of the large energy-producing eddies. The small eddies are characterized by the Kolmogorov scale of

time, $\sqrt{\nu/\varepsilon}$.

Two-equation turbulence models have the capability of predicting more complex flows than zero and one-equation models, since both the velocity and length scales are solved locally. Two-equation models are, however, based on the assumption that the Boussinesq approximation is valid and the turbulence is isotropic. The low Reynolds number $k-\varepsilon$ formulation of two-equation turbulence models has been widely adopted in practical engineering problems due to its robustness. The low Reynolds number form is chosen for its more rigorous near-wall treatment of turbulent quantities (Patel et al., 1985).

The major drawback of the $k-\varepsilon$ model is probably the near-wall formulation which fails to reproduce correctly the effects of the solid boundary on turbulence. Several models have been developed in an attempt to improve near-wall modeling. Such models have been examined by Patel et al.(1985), who concluded that the models of Launder and Sharma (1974), Chien (1982), Lam and Bremhorst (1981), and Wilcox and Rubensin (1980) performed better than the others did. The Jones-Launder model (1972) and Launder-Sharma model (1974) of the low Reynolds number $k-\varepsilon$ models have been applied to several complex engineering problems and found to be more stable in nearly all calculations. In addition, the damping functions and the low Reynolds number terms are explicit functions of y^+ in these models. Gerolymos (1990) made comparisons using the Launder-Sharma turbulence model with experimental data for three shock-wave/turbulent-boundary-layer interaction flows, and obtained globally satisfactory results except for flows in important streamline curvature. Sahu and Danberg (1986) computed an axisymmetric bump flow using the thin-layer Navier-Stokes equation and the Chien turbulence model (1982), and predicted a much sharper rise in skin friction in the flow redevelopment region. Another $k-\varepsilon$ turbulence model was proposed by Abe et al. (1994), whose main improvement was the employment of the Kolmogorov velocity scale $(\nu\varepsilon)^{1/4}$, instead of the conventional friction velocity u_τ. Eventually, the dimensionless distance y^* replaced the dimensionless distance y^+. Their model performed well in solving a diffuser flow with a strong adverse pressure gradient, flow separation and the reattachment of a backward-facing step because y^* might be well defined near the flow separation zone where the wall shear stress is zero. This model appreciates the motion of small-scale eddies which dissipate the kinetic energy to heat by the action of molecular viscosity that is independent of the relatively slow motion of the large eddies and the mean flow. These motions of the mean flow and the large eddy account for most of the transport of properties in a turbulent flow and have been the main consideration in developing a typical turbulence closure. Wilcox (1993) tested several low Reynolds number $k-\varepsilon$ models and the $k-\omega$ model by computing the boundary layer with various pressure gradients. The $k-\omega$ model predicted skin friction coefficient more accurately for strong adverse pressure gradient flows. For the $k-\omega$ model, however, the freestream value of ω produced some affects on boundary layers (Menter, 1991). Yoon et al. (1994) also tested various low Reynolds number $k-\varepsilon$ models and the $k-\omega$ turbulence model using the verified upwind scheme for the compression corner flow. The Launder-Sharma $k-\varepsilon$ model (1974) and the Wilcox $k-\omega$ model (1993) performed better than the others did in predicting the pressure and skin friction coefficient distributions along the wall of the corner. Further, Yoon et al.(1994) studied scheme dependent solutions. Three different centered schemes and an upwind scheme were tested with the Baldwin-Lomax model. It was found that the upwind scheme gave much better predictions than the other schemes.

In the meantime, the finite-difference or finite-volume methods based on upwind flux difference splitting have been developed by various researchers. Upwind method is appropriate due to its robustness in capturing the shock-wave in the transonic/supersonic flow. Classical upwind schemes can roughly be divided into two categories: flux vector splitting schemes of Steger-Warming (1981) and Van Leer (1982), and flux difference splitting schemes of Godunov (1959),

Roe (1981), and Osher (1984). In the original Godunov scheme, the local Riemann problem is solved exactly; whereas, Roe (1981) and Osher (1984) used approximate Riemann solvers instead. Among the upwind flux difference splitting Navier-Stokes methods, Lombard et al.(1983) solved the 2-D/3-D complex high speed flows quite efficiently with reasonable accuracy using the Conservative Supra Characteristic Method (CSCM). The CSCM type of upwind flux difference splitting scheme has the merits of the upwind scheme, the ease of applying characteristic boundary conditions, and the robust flow solver. For the ARL-SL19 supersonic compressor cascade flows, Kim et al.(1996) successfully studied the effects of passive control of shock-wave/boundary-layer interaction on the cascade using various size cavities, and Song et al.(2001) investigated the flow characteristics of supersonic compressor cascade with various turbulence models. Song et al.(1998) reported the off-design performance of centrifugal compressor diffusers with various massflow rates using the CSCM type of upwind method.

In this work, we developed the CSCM type-fully coupled, upwind Navier-Stokes code with three two-equation turbulence models including Abe et al.(1994), and showed the results of a comparative study on the performance of an algebraic equation and selected two-equation turbulence models in predicting the compressible, turbulent transonic/supersonic flows.

2. Governing Equations and Turbulence Closure

Turbulence models compared in this study are the Baldwin-Lomax algebraic model (1978), the Launder-Sharma (1974), Abe et al.(1994), and Wilcox (1993) models. The Favre averaged two-dimensional Navier-Stokes equation with a two-equation model can be written as

$$\frac{\partial q}{\partial t}+\frac{\partial F}{\partial x}+\frac{\partial G}{\partial y}=\frac{\partial F_v}{\partial x}+\frac{\partial G_v}{\partial y}+S \qquad (1)$$

with

$$q=\begin{bmatrix}\rho\\ \rho u\\ \rho v\\ E\\ \rho k\\ \rho\phi\end{bmatrix},\ F=\begin{bmatrix}\rho u\\ \rho u^2+p\\ \rho uv\\ u(E+p)\\ \rho uk\\ \rho u\phi\end{bmatrix},\ G=\begin{bmatrix}\rho v\\ \rho uv\\ \rho v^2+p\\ v(E+P)\\ \rho vk\\ \rho v\phi\end{bmatrix} \qquad (2)$$

$$F_v=\begin{bmatrix}0\\ \tau_{xx}\\ \tau_{xy}\\ u\tau_{xx}+v\tau_{xy}-Q_x\\ \left(\mu+\frac{\mu_t}{\sigma_k}\right)\frac{\partial k}{\partial x}\\ \left(\mu+\frac{\mu_t}{\sigma_\phi}\right)\frac{\partial \phi}{\partial x}\end{bmatrix},\ G_v=\begin{bmatrix}0\\ \tau_{yx}\\ \tau_{yy}\\ u\tau_{yx}+v\tau_{yy}-Q_y\\ \left(\mu+\frac{\mu_t}{\sigma_k}\right)\frac{\partial k}{\partial y}\\ \left(\mu+\frac{\mu_t}{\sigma_\phi}\right)\frac{\partial \phi}{\partial y}\end{bmatrix} \qquad (3)$$

The effective stress tensor and the effective heat flux vector are given by

$$\tau_{ij}=(\mu+\mu_t)\left[\left(\frac{\partial u_i}{\partial x_j}+\frac{\partial u_j}{\partial x_i}\right)-\frac{2}{3}\delta_{ij}\frac{\partial u_m}{\partial x_m}\right]-\frac{2}{3}\delta_{ij}\rho k \qquad (4)$$

$$Q_i=-C_p\left(\frac{\mu}{\mathrm{Pr}_l}+\frac{\mu_t}{\mathrm{Pr}_t}\right)\frac{\partial T}{\partial x_i} \qquad (5)$$

For the $k-\varepsilon$ turbulence model, the source term vector is given by

$$S=\begin{bmatrix}0\\ 0\\ 0\\ 0\\ P_k-\rho\phi+L_k\\ c_1f_1\frac{\phi}{k}P_k-c_2f_2\frac{\rho\phi^2}{k}+L_\phi\end{bmatrix} \qquad (6)$$

Model constants and the definitions of the low Reynolds number terms are given in Table 1. In the model of Abe et al.(1994), the constants were changed by the relation, $c_1\simeq c_2-\kappa(\sigma_\varepsilon\sqrt{c_\eta})$, as proposed in their paper. The damping functions for the respective model are listed in Table 2. The turbulence kinetic energy production and the eddy viscosity are given by

$$P_k=\mu_t\left[\frac{1}{2}\left(\frac{\partial u_i}{\partial x_j}+\frac{\partial u_j}{\partial x_i}\right)^2-\frac{2}{3}\left(\frac{\partial u_m}{\partial x_m}\right)^2\right]-\frac{2}{3}\rho k\frac{\partial u_m}{\partial x_m} \qquad (7)$$

$$\mu_t=c_\eta f_\eta\rho\frac{k^2}{\phi} \qquad (8)$$

The effects of compressibility due to the density

Table 1 Model constants and dissipation rates

Model	ϕ	σ_k	σ_ϕ	c_1	c_2	L_k	L_ϕ
Launder-Sharma (1974)	$\tilde{\varepsilon}$	1.0	1.3	1.44	1.92	$-2\mu\left(\frac{\partial\sqrt{k}}{\partial x_j}\right)^2$	$2\frac{\mu\mu_t}{\rho}\left(\frac{\partial^2 u_i}{\partial x_j \partial x_m}\right)^2$
Abe et al.(1994)	ε	1.9	1.9	1.6	1.9	0	0

Table 2 Damping functions

Model	f_η	f_1	f_2
Launder-Sharma (1974)	$1-0.3\exp(-R_t^2)$	1.0	$\exp\left(\frac{-3.4}{(1+0.02R_t)^2}\right)$
Abe et al. (1994)	$[1-\exp(-y^*/14)]^2$ $\times[1+(5/R_t^{3/4})\exp[-(R_t/200)^2]]$	1.0	$[1-\exp(-y^*/3.1)]^2$ $\times[1-0.3\exp[-(R_t/6.5)^2]]$

fluctuations are not considerable in the range of Mach number where the Morkovin hypothesis is valid (Morkovin, 1964), and the applicability of the turbulence closure is restricted below the hypersonic flow regime.

For the $k-\omega$ turbulence model, the source term vector is given by

$$S=\begin{bmatrix}0\\0\\0\\0\\P_k-\beta^*\rho\omega_k\\ \alpha\frac{\omega}{k}P_k-\beta\rho\omega^2\end{bmatrix} \tag{9}$$

where $\beta=3/40$, $\beta^*=0.09$, $\sigma_k=2.0$, $\sigma_\omega=2.0$, $\alpha=5/9$, and $\gamma^*=1$.

The eddy viscosity of the $k-\omega$ model is

$$\mu_t=\rho\gamma^*\frac{k}{\omega} \tag{10}$$

3. Numerical Methods

The CSCM upwind flux difference splitting method utilizes the properties of similarity transformation based on the conservative, the primitives and the characteristic variables:

$$\begin{aligned}\Delta F=A\Delta q&=MT\Lambda T^{-1}M^{-1}\Delta q\\&=MT\Lambda T^{-1}\Delta\tilde{q}=MA'\Delta\tilde{q}\\&=MT\Lambda\Delta\tilde{\tilde{q}}\end{aligned} \tag{11}$$

where Λ is a diagonal matrix whose diagonal elements correspond to the eigenvalues (u, u, $u+a$, $u-a$, u, u), and variables q, $\tilde{q}$, $\tilde{\tilde{q}}$, and are related as follows:

$$\Delta q=M^{-1}\Delta\tilde{q},\ \Delta\tilde{\tilde{q}}=T^{-1}\Delta\tilde{q} \tag{12}$$

T^{-1} is somewhat arbitrary as to scaling that leads to logarithmic difference approximations for density, pressure, and Mach number.

The characteristic variables can be obtained from the primitive variables through the following relation

$$T^{-1}(A'\Delta\tilde{q})=T^{-1}(T\Lambda T^{-1})\Delta\tilde{q}=\Lambda\Delta\tilde{\tilde{q}} \tag{13}$$

The inviscid flux ΔF can be divided into ΔF^+ and ΔF^- using diagonal truth function matrix $D^\pm$ and Eq. (11) can be written as

$$\Delta F=MT(D^+ +D^-)\,T^{-1}A'\Delta\tilde{q}=\Delta F^+ +\Delta F^- \tag{14}$$

where $D^+=\frac{1}{2}\left(1+\frac{\Lambda}{|\Lambda|}\right)$ and $D^-=\frac{1}{2}\left(1-\frac{\Lambda}{|\Lambda|}\right)$.

Using the relation $A'\Delta\tilde{q}=\tilde{M}^{-1}\Delta q$, the above equation can be rewritten as

$$\Delta F^\pm=MTD^\pm T^{-1}\tilde{M}^{-1}\Delta q=A^\pm\Delta q \tag{15}$$

Equation (15) satisfies the property 'U' of Roe (1985) and thus the flux vectors are conserved. Although the formulation becomes complicated due to transformation matrices M, T, and $\tilde{M}^{-1}$, the differencing scheme, in turn, represents the convective flow propagation through these matrices and naturally allows easy characteristic boundary conditions via the modified T'^{-1}.

The implicit finite difference equation can be discretized using one-side differencing depending on the sign of eigenvalues of the Jacobian matrices. For second order accuracy of the inviscid terms in the explicit part on the right-hand side, we use the Fromm scheme with the minmod limiter (Hirsch, 1989). The RHS of a direction can be written as

$$RHS_i = -A^+\Delta q_{i-1} - A^-\Delta q_i - \frac{1}{4}[\text{minmod}(A^-\Delta q_{i-1}, 3A^-\Delta q_i) - \text{minmod}(A^-\Delta q_{i+1}, 3A^-\Delta q_i)] - \frac{1}{4}[\text{minmod}(A^+\Delta q_i, 3A^+\Delta q_{i-1}) - \text{minmod}(A^+\Delta q_{i-2}, 3A^+\Delta q_{i-1})] \quad (16)$$

Using approximate factorization (Beam and Warming, 1976), the equations are solved along ξ-direction and then n-direction successively. We consider that the converged solutions are obtained when the L^2 norm of the residuals of all variables reaches 1.0×10^{-5}.

4. Grid System and Boundary Conditions

The grid system was generated by using elliptic P.D.E. grid techniques. A stretching function was used to cluster most grid points near the wall, which is able to resolve to high transverse flow gradients in the boundary layer. The viscous mesh employed a first-gridpoint placement from the wall at y^+ less than unit. The grid system was 100×60 over the axisymmetric bump in the longitudinal and normal directions, respectively. The same configuration was used experimentally by Johnson et al.(1982). The incoming flow properties were prescribed by freestream values. Also, the 90×70 grid system was constructed over the compression ramp. The incoming flow properties were prescribed using the solutions of the flat plate turbulent flow. In both cases, a first-order extrapolation was used at outflow boundaries, and the no-slip and adiabatic conditions were imposed on the wall surfaces. In the two-equation model, the turbulent kinetic energy was set to zero on the wall. The wall dissipation rate for respective models is given in Table 3. Figure 1 shows the grid dependence of the skin friction coefficient along the wall surface for the compression-corner flow. The results indicates that the number of grid points used in current study was sufficient to resolve the shock/boundary layer interaction and verify the performance of turbulence models in terms of the skin friction coefficient because little change was noted for a near doubling of the number of grid points in the vicinity of this value.

Table 3 Wall boundary conditions of dissipation rate

Model	Variable	Value
Launder-Sharma (1974)	$\tilde{\varepsilon}$	0
Abe et al.(1994)	ε	$\frac{2\nu k_1}{y_1^2}$ or $\nu\left(\frac{\partial\sqrt{k}}{\partial y}\right)^2$
Wilcox (1993)	ω	$\frac{6\nu}{\beta y^2}$ as $y\to0$

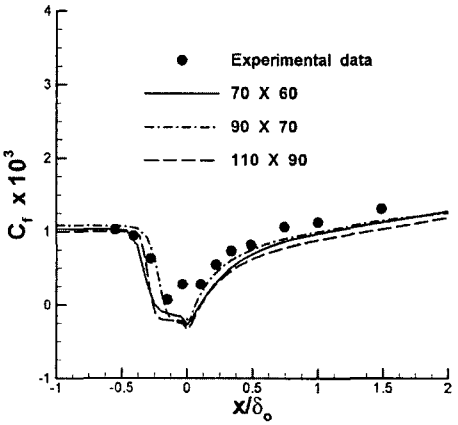

Fig. 1 Dependence of the skin friction coefficient for the 16° ramp flow on number of the grid points

5. Results and Discussion

For the validation of the code, we compared the laminar solution with experimental data for a planar nozzle reported by Mason, et al.(1980) The inlet Mach number was taken as 0.232 and Reynolds number was 7.5×10^6 based on the inlet half-height. In Fig. 1, the pressure distributions along the wall and the centerline in the down-

stream direction are compared with the experimental data, which were taken at the midspan of the duct walls and on the centerline of the endwalls. The agreement between the numerical results and the experimental data seems to be excellent along both the nozzle wall and the centerline positions.

For the evaluation of the current upwind scheme to predict the transonic/supersonic flowfield with the inviscid-viscous interaction and the shock-wave/turbulent-boundary-layer interactio n, we employed the Baldwin-Lomax model (BL), low Reynolds number $k-\varepsilon$ models of Launder and Sharma (LS), Abe et al.(AN), and the $k-\omega$ model of Wilcox (WC) for turbulence closure.

5.1 Flat plate flow

The supersonic turbulent flow over the flat plate at $Ma_\infty=2.83$ was studied as a first-test case. Comparisons of numerical results were carried out with the traditional velocity profile of So et al.(1994) for a turbulent boundary layer. The von Karman constant, κ, was assumed to be a constant value of approximately 0.41 for flat plate compressible boundary layers with freestream Mach number below 5 and adiabatic wall boundary conditions, even if κ could be changed depending on the Mach number and the total heat flux for compressible flows. Figure 2 shows that the mean velocity profiles are consistent with the logarithmic velocity profile. It is encouraging that the level of agreement is similar to the one in the previous investigation (Coakly et al., 1992).

5.2 Transonic bump flow

Next, the strong, transonic, inviscid-viscous interaction over the axisymmetric-bump model as shown in Fig. 3 was chosen for the evaluations of the turbulence models. The freestream Mach number was 0.875 and the Reynolds number based on the length of the bump was 2.761×10^6. The general characteristics of the axisymmetric turbulent flow field over the bump were compared among the experimental data of Bachalo and Johnson(1979) and the results from four different turbulence models. Figure 4 shows the dimensionless pressure contours in the flow field near the bump. We can see that after the flow acceleration over the front portion of the bump,

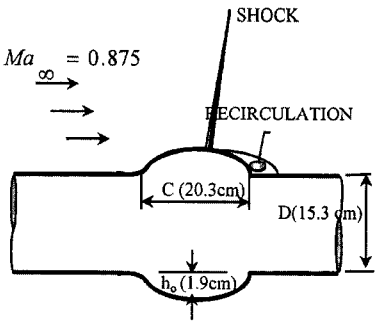

Fig. 3 Schematic diagram of an axisymmetric bump flow at $Ma_\infty=0.875$

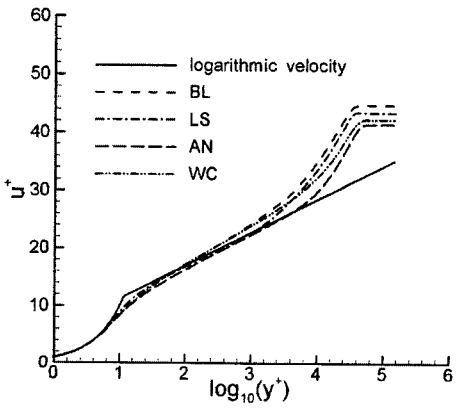

Fig. 2 Logarithmic velocity profiles for the compressible flat plate flow at $Ma_\infty=2.83$

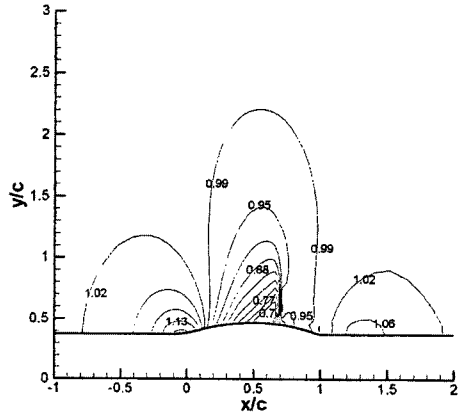

Fig. 4 Dimensionless pressure contours over the axisymmetric bump

the shock-wave occurred at the aft portion of the bump which was clearly predicted by current numerical method.

Figure 5 depicts the dimensionless surface pressure distributions along the wall. The wall pressure value of each model is similar to each other until it encounters the compression wave at about $x/c=-0.3$. Because of the flow acceleration downstream of bump leading edge, the pressure decreases almost linearly before the weak shock-wave occurs. Flow accelerates to a low supersonic flow. Then, the pressure increases sharply after a weak shock-wave occurs at about $x/c=0.6$. The experimental data reveal a small 'plateau' of pressure distribution near $x/c=1$, partly due to the flow separation in the strong inviscid-viscous flow interaction region. When the mean flow field is suddenly distorted due to the shock-wave, the eddy-viscosity models tend to predict sudden changes in both the Reynolds shear stress and the eddy viscosity level. That is why these models could have some deficiencies in predicting inviscid-viscous interaction near the flow separation zone (Johnson and King, 1985). However, the result of the AN model was consistent with the experimental data.

The skin friction coefficient distribution along the wall surface is shown in Fig. 6. The strength of shock-wave is not sufficient to produce a flow separation right after the weak shock-wave. However, the combination of the perturbation permeated into the boundary layer by the shock-wave and the adverse pressure gradient over the second half of the bump, due to diffuser effect, causes the flow separation near $x/c=0.7$. The BL model shows that the location and the size of flow separation are similar to the experimental data; however, it severely underpredicted the values in the redeveloping flow region than did the two-equation models. The two-equation models, on the other hand, predicted the location of flow separation further downstream than the experiment did.

Reynolds shear stress distributions across the normal direction at several streamwise stations are compared with the measured data in Fig. 7. The oblique shock-wave which yields the defect of the velocity profile has a very strong influence on shear stress which increases rapidly and exceeds the experimental result just downstream of the shock-wave. However, most models predicted the profiles well in qualitative consistency with the experimental data. Additionally, the shear-stress peak shifts away from the wall along the streamwise direction as shown in experimental data. The BL and LS models predicted the sudden increase in the shear-stress near the shear layer downstream of the shock wave, whereas the AN model revealed the slow increase in the shear stress along streamwise direction in the flow-reversal region, which was able to produce the reasonable size of the separation bubble near the end of the bump. The WC model overpredicted

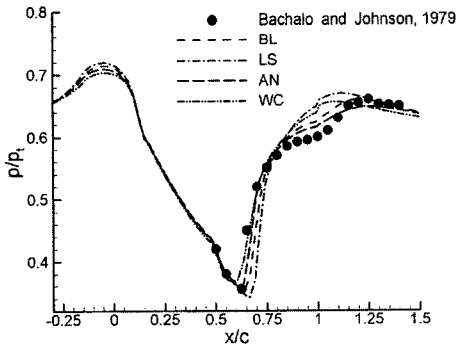

Fig. 5 Wall pressure distribution showing comparison of the current results with the experimental data of Bachalo and Johnson (1979) for the axisymmetric bump

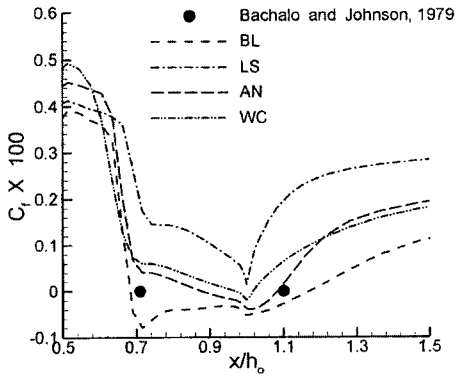

Fig. 6 Skin friction coefficient distribution over the axisymmetric bump

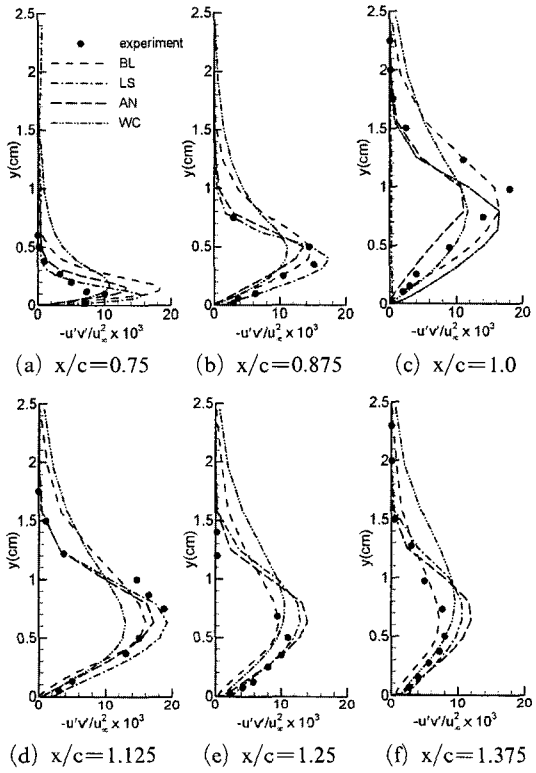

Fig. 7 Predicted Reynolds shear stress profiles compared with experimental data of Bachalo and Johnson (1979) for the axisymmetric bump

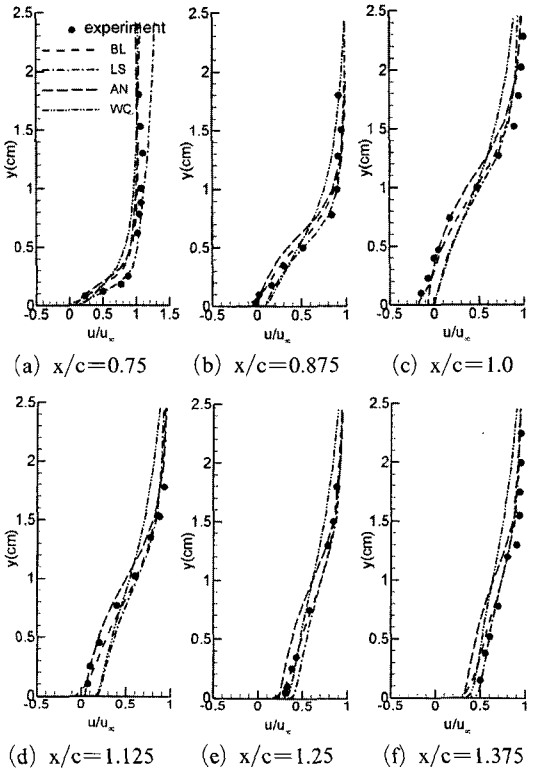

Fig. 8 Predicted mean velocity profiles compared with experimental data of Bachalo and Johnson (1979) for the axisymmetric bump

the values of the shear stress at about 1.5 cm from the wall, which has consistent with Menter's observation (Menter, 1991 and 1994) that specifying freestream value of ω had significant effect on the boundary layer thickness.

Measured and computed velocity profiles over the aft portion and just downstream of the bump are shown in Fig. 8. All velocity profiles showed good agreements with the experiment, and the BL and the AN models, in particular, performed better than the other models. Although the AN model predicted lower shear stress over the reverse flow zone, the predicted velocity profiles were in better agreement with the experimental data. The other two-equation models also performed well in predicting the boundary layer near the separation zone. The LS model produced reasonable velocity profiles for the redevelopment of boundary layer, whereas it failed to predict the flow separation around the aft portion of the bump.

5.3 Supersonic compression ramp

The last comparison in the present study is made for a compression corner case to investigate the interactions between shock-waves and turbulent-boundary-layers as shown in Fig. 9. The freestream Mach number was 2.85 and the Reynolds number based on the incoming boundary layer thickness was 1.6×10^6. The experimental data by Settles et al. (1979) were compared with the current numerical results. Figure 10 shows the dimensionless pressure contour over the ramp. The shock-wave was clearly predicted with the shock-wave angle 37° which corresponded to the oblique shock relations with the deflection angle 16°.

Figure 11 depicts the surface pressure distribution along the wall. The wall pressure is identical to the freestream value until the oblique shock-

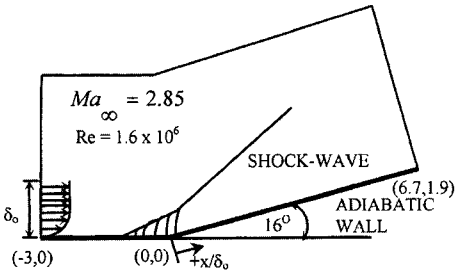

Fig. 9 Schematic diagram of the 16° ramp flow at Ma_∞=2.85

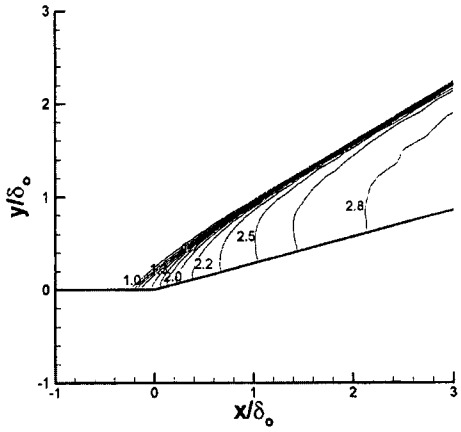

Fig. 10 Dimensionless pressure contours over the 16° ramp

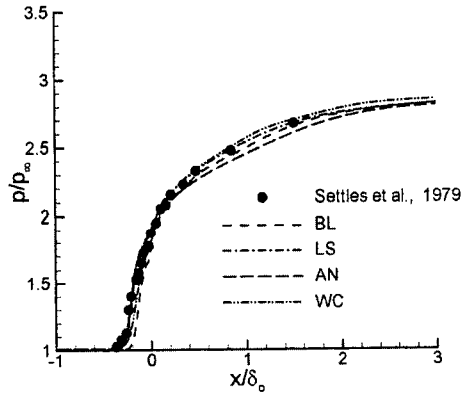

Fig. 11 Wall pressure distribution showing comparison of the current results with the experimental data of Settles et al. (1979) for the 16° ramp

wave occurs at about $x/\delta_o = -0.3$. The pressure gradient decreased downstream of the corner and the pressure eventually reached a level of

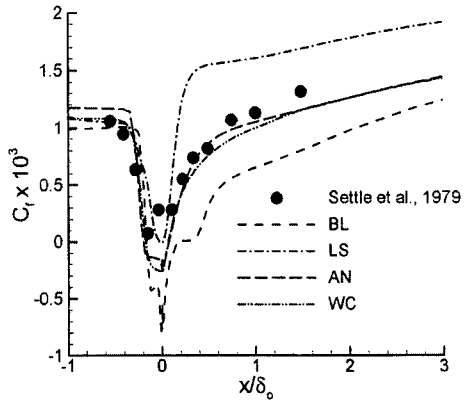

Fig. 12 Skin friction coefficient distribution showing comparison of the current results with the experimental data of Settles et al. (1979) for the 16° ramp

theoretical inviscid pressure rise, as expected (Muck and Smits, 1983). The BL model exhibits a kink near the corner indicating the presence of flow separation. All models are highly consistent with the experimental data.

The skin friction coefficient distribution along the surface is shown in Fig. 12. The skin friction coefficients from the BL and the two-equation models are in reasonably good agreement with the experimental data in the forward portion of the sharply decreasing skin friction coefficient. However, the BL model severely underpredicted the skin friction values downstream of the corner, while the LS model produced high skin friction values in this region. The WC and the AN models predicted the skin friction successfully in the redevelopment region. The two-equation models using y^+ in the damping functions and the low Reynolds number terms appearing in the Chien and the Nagano-Tagawa models (Yoon et al., 1994) easily show a much more rapid rise of the skin friction values in the redevelopment region compared to the experimental data. This is due to a significantly larger eddy viscosity, as indicated by Sahu et al. (1986) and Yoon et al. (1994). We notice, however, the AN model, which uses y^* instead of y^+, produced agreeable skin friction values after the shock-wave.

Reynolds shear stress distributions are compared with the measurement data (Muck et al.,

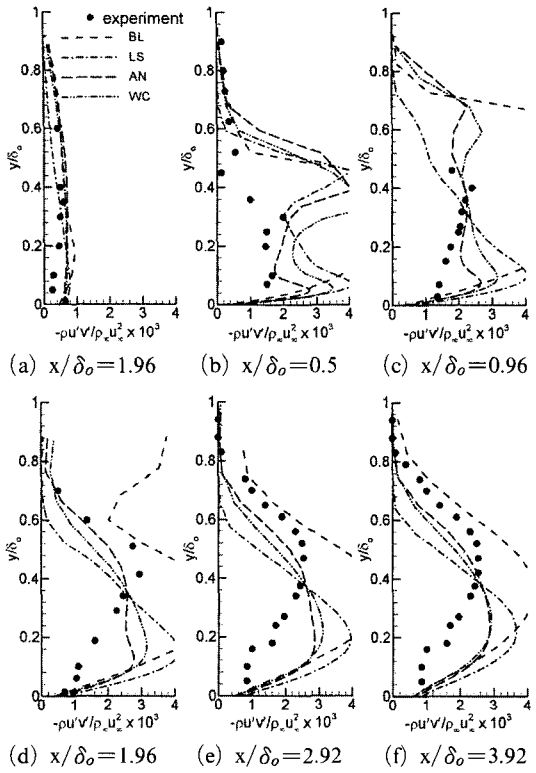

(a) $x/\delta_o=1.96$ (b) $x/\delta_o=0.5$ (c) $x/\delta_o=0.96$

(d) $x/\delta_o=1.96$ (e) $x/\delta_o=2.92$ (f) $x/\delta_o=3.92$

Fig. 13 Predicted Reynolds shear stress profiles compared with experimental data of Settles et al. (1979) for the 16° ramp

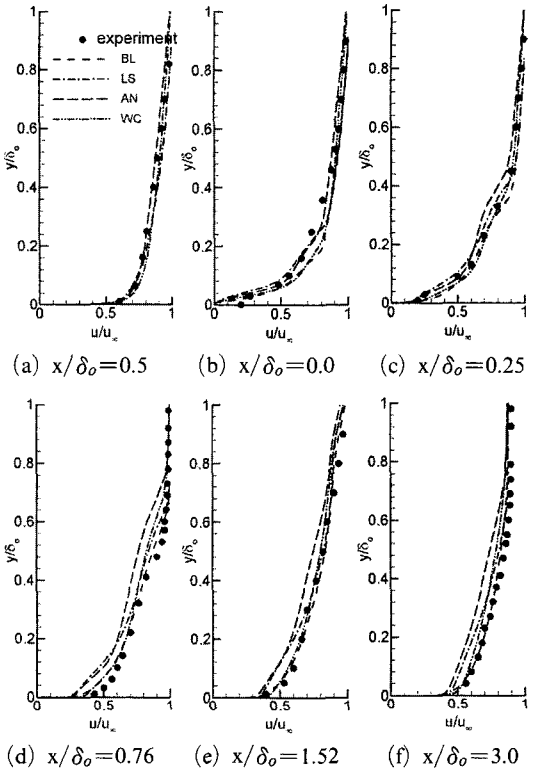

(a) $x/\delta_o=0.5$ (b) $x/\delta_o=0.0$ (c) $x/\delta_o=0.25$

(d) $x/\delta_o=0.76$ (e) $x/\delta_o=1.52$ (f) $x/\delta_o=3.0$

Fig. 14 Predicted mean velocity profiles compared with experimental data of Settles et al. (1979) for the 16° ramp

1983 ; Smits et al., 1987) in Fig. 13. Ahead of the shock-wave, the peak value of the shear stress was close to the wall. The oblique shock-wave had a very strong influence on the shear stress which became more distorted and had much bigger value of the peak in the profile, and its peak moved away from the wall. None of the two-equation models could successfully predict the sudden changes in the turbulence structure through the shock-wave which penetrated the boundary layer. The results from the AN model were qualitatively similar to those of the WC model.

Comparisons of the velocity profiles at several locations along the surface are shown in Fig. 14. Upstream of the shock-wave, all computed results were found to be similar to those which were obtained experimentally. Nevertheless, the BL model predicted the broad flow reversal and the excessive shear stresses downstream of the shock-wave, velocity profiles from the BL model showed the good agreement with the experimental data. However, the two-equation models predicted the narrow reversed flow region and yielded that the redevelopment of the boundary layer was somewhat slow downstream of the reattachment portion. The AN model which produced the smallest peak of the shear stress in redeveloped regions revealed the large deviation of the velocity profiles from the experimental data.

6. Conclusions

In this paper a compressible upwind flux difference splitting Navier-Stokes code using four turbulence models was developed. Each model's performance in predicting the turbulent transonic/supersonic flow was evaluated. The $k-\varepsilon$ model of Abe et al. of the two-equation models performed well in predicting the wall pressure distribution and the velocity profiles in the re-

verse flow zone over the axisymmetric bump, even though there were some discrepancies with the experimental data in the shear-stress distributions. This model predicted excellent skin friction coefficient as Wilcox's model did in supersonic compression ramp flow. Though Wilcox's model showed the sensitivity of the solution to the freestream value of the specific dissipation rate, this model was superior to other models with regard to numerical stability. The two-equation models revealed that the redevelopment of the boundary layer was somewhat slow downstream of the reattachment portion.

Acknowledgment

The authors wish to thank to Prof. Akira Nakayama for his general support while the first author stayed at Shizuoka University.

References

Abe K., Nagano, Y. and Kondoh, T., 1994, "A New Turbulence Model for Predicting Fluid Flow and Heat Transfer in Separating and Reattaching Flows −1, Flow Field Calculation," *International Journal of Heat and Mass Transfer*, Vol. 37, No. 1, pp. 139~151.

Bachalo, W. D. and Johnson, D. A., 1979, "An Investigation of Transonic Turbulent Boundary Layer Separation Generated on an Axisymmetric Flow Model," *AIAA Paper* 79-1479.

Baldwin, B. S. and Lomax, H., 1978, "Thin Layer Approximation and Algebraic Model for Separated Turbulent Flows," *AIAA Paper* 78-257.

Cebeci, T. and Smith, A. M. O., 1974, "Analysis of Turbulent Boundary Layers," *Series in Applied Mathematics and Mechanics*, Vol. XV, Academic Press.

Chien, K. Y., 1982, "Prediction on Channel and Boundary-Layer Flows with a Low-Reynolds-Number Turbulence Model," *AIAA Journal*, Vol. 20, No. 1, pp. 33~38.

Coakly, T. J. and Huang, P. G., 1992, "Turbulence Modeling For High Speed Flows," *AIAA Paper* 92-0436.

Gerolymos, G. A., 1990, "Implicit Multiple-Grid Solution of the Compressible Navier-Stokes Equations Using Turbulence Closure," *AIAA Journal*, Vol. 28, No. 11, pp. 1707~1717.

Godunov, S. K., 1959, "A Finite Difference Method for the Numerical Computation of Discontinuous Solutions of the Equations of Fluid Dynamics," Mat. Sbornik, Vol. 47, pp. 271~290.

Goldberg, U. C., 1991, "Derivation and Testing of a One-Equation Model Based on Two Time Scales," *AIAA Journal*, Vol. 29, No. 8, pp. 1337~1340.

Grasso, F. and Falconic, D., 1993, "High-Speed Turbulence Modeling of Shock-Wave/Boundary-Layer Interaction," *AIAA Journal*, Vol. 31, No. 7, pp. 1199~1206.

Hirsch, C., 1989, "Numerical Computation of Internal and External Flows," Vol. 2, JOHN WILEY & SONS, NY, pp. 493~594.

Johnson, D. A., Horstman, C. C. and Bachalo, W. D., 1982, "Comparison Between Experiment and Prediction for a Transonic Turbulent Separated Flow," *AIAA Journal*, Vol. 20, No. 4, pp. 737~744.

Johnson, D. A. and King, L. S., 1985, "A Mathematically Simple Turbulence Closure Model for Attached and Separated Turbulent Boundary Layers," *AIAA Journal*, Vol. 23, No. 11, pp. 1684~1692.

Jones, W. P. and Launder, B. E., 1972, "The Prediction of Laminarization with a Two-Equation Model of Turbulence," *International Journal of Heat and Mass Transfer*, Vol. 15, No. 2, pp. 301~314.

Kim, S. D., Kwon, C. O., Song, D. J. and Sa, J. Y., 1996, "Performance Enhancement Study Using Passive Control of Shock-Boundary Layer Interaction in a Transonic/Supersonic Compressor Cascade," *Transactions of KSME*, Vol. 20, No. 9, pp. 2944~2952.

Lam, C. K. and Bremhorst, K., 1981, "A Modified Form of the $k-\varepsilon$ Model for Predicting Wall Turbulence," *ASME Journal of Fluids Engineering*, Vol. 103.

Launder, B. E. and Sharma, B. I., 1974, "Application of the Energy Dissipation Model of Turbulence to the Calculation of Flows near a

Spinning Disk," *Letters in Heat and Mass Transfer*, Vol. 1, No. 2, pp. 131~138.

Lombard, C. K., Bardina, J., Venkatapathy, E. and Oliger, J., 1983, "Multi-dimensional Formulation of CSCM-An Upwind Flux Difference Eigenvector Split Method for the Compressible Navier-Stokes Equations," *AIAA Paper* 83-1859.

Mason, M. L., Putnam, L. E. and Re, R. J., 1980, *The Effect of Throat Contouring on Two-Dimesional Converging-Diverging Nozzles at Static Conditions*, NASA Technical Paper 1704.

Menter, F. R., 1992, "Influence of Freestream Values on Turbulence Model Predictions," *AIAA Journal*, Vol. 30, No. 6, pp. 1657~1659.

Menter, F. R., 1994, "Two-Equation Eddy-Viscosity Turbulence Models for Engineering Applications," *AIAA Journal*, Vol. 32, No. 8, pp. 1598~1605.

Morkovin, M. V., 1962, "Effects of Compressibility on Turbulent Flows," *The Mechanics of Turbulence*, A. Favre, Ed., Gordon and Breach, p. 367.

Muck, K. C. and Smits, A. J., 1983, "The Behaviour of a Compressible Turbulent Boundary Layer under Incipient Separation Conditions," in Turbulent Shear Flow, Vol. 4, Spring-Verlag, Berlin Heidelberg, pp. 235~245.

Osher, S., 1984, "Riemann Solvers, the Entropy Condition, and Difference Approximations," *SIAM Journal of Numerical Analysis*, Vol. 21, No. 2, pp. 217~235.

Patel, V. C., Rodi, W. and Scheuere, G., 1985, "Turbulence Models for Near-Wall and Low-Reynolds-Number Flows: A Review," *AIAA Journal*, Vol. 23, No. 9, pp. 1308~1319.

Roe, P. L., 1981, "The Use of the Riemann Problem in Finite-Difference Schemes," Proceedings of the 7th International Conference on Numerical Methods in Fluid Dynamics, Lecture Notes in Physics, Vol. 141, pp. 354~359.

Sahu, J. and Danberg, J. E., 1986, "Navier-Stokes Computations of Transonic Flows with a Two-Equation Turbulence Model," *AIAA Journal*, Vol. 24, No. 11, pp. 1744~1751.

Sarkar, S., Erlebacher, G., Hussaini, M. Y. and Kreiss, H. O., 1990, "The Modeling of Turbulent Dissipation in Compressible Turbulence," in Engineering Turbulence Modeling and Experiments, ed. Rodi & Ganic, Elsevier, pp. 109~118.

Settles, G. S., Fitzpatrick, T. J. and Bogdonoff, S. M., 1979, "Detailed Study of Attached and Separated Compression Corner Flowfields in High Reynolds Number Supersonic Flow," *AIAA Journal*, Vol. 17, No. 6, pp. 579~585.

Shyy, W., Thakur, S. S., Ouyang, H., Liu, J. and Blosch, E., 1997, Computational Techniques for Complex Transport Phenomena, Cambridge University Press, Cambridge.

Smits, A. J. and Muck, K. C., 1987, "Experimental Study of Three Shock Wave/Turbulent Boundary Layer Interactions," *Journal of Fluid Mechanics*, Vol. 182, pp. 291~314.

So, R. M. C., Zhang, H. S., Gataki, T. B. and Speziale, C. G., 1994, "Logarithmic Laws for Compressible Turbulent Boundary Layers," *AIAA Journal*, Vol. 32, No. 12, pp. 2162~2168.

Song, D. J., Kim, S. D., Kwon, C. O. and Seo, J. I., 1998, "A Computational Off-Design Performance Analysis of Centrifugal Compressor Diffusers," *Computational Fluid Dynamics Journal*, Vol. 6, No. 9, pp. 549~560.

Song, D. J., Hwang, H. C. and Lee, Y. I., 2001, "A Numerical Study of Shock Wave/Boundary Layer Interaction in a Supersonic Compressor Cascade," *KSME International Journal*, Vol. 15, No. 3, pp. 366~373.

Steger, J. L. and Warming, R. F., 1981, "Flux Vector Splitting of the Inviscid Gasdynamics Equations with Application to Finite Difference Methods," *Journal Computational Physics*, Vol. 40. No. 2, pp. 263~293.

Van Leer B., 1982, "Flux-Vector Splitting for Euler Equations," *Proceedings of the 8th International Conference on Numerical Methods in Fluid Dynamics*, Lecture Notes in Physics, Vol, 170, Springer-Verlag, Berlin, pp. 507~512.

Visbal, M. and Knight, D., 1984, "The Baldwin-Lomax Turbulence Model for Two-Dimensional Shock-wave/Boundary-Layer Interactions," *AIAA Journal*, Vol. 22, No. 5, pp. 921~928.

Warming, R. F. and Beam, R. M., 1976, "An Implicit Finite-Difference Algorithm for Hyperbolic Systems in Conservation Law Form," *Jour-*

nal of Computational Physics, Vol. 22, No. 1, pp. 87~110.

Wilcox, D. C., 1993, "Comparison of Two-Equation Turbulence Models for Boundary Layers with Pressure Gradient," *AIAA Journal*, Vol. 31, No. 9, pp. 1414~1421.

Wilcox, D. C. and Rubesin, M. W., 1980, *Progress in Turbulence Modeling for Complex Flowfields Including the Effects of Compressibility*, NASA TP 1517.

Yoon, B. K., Chung, M. K. and Park, S. O., 1995, "A Computational Study on Shock-wave/Turbulent-boundary-layer Interaction with Two-equation Turbulence Models," *AIAA Paper* 94-2276.